Removal of Uranium(VI) from Aqueous Solution by Iron Nanoparticles Synthesized from Testa Extract of *Annacardium occidentale*: A Fluorimetric Study

CH CHANDRA, FAHMIDA KHAN[*], SONALIKA AGRAWAL and VIPIN KUMAR SONI

Department of Chemistry, National Institute of Technology, Raipur-492010, India

*Corresponding author: E-mail: fkhan.chy@nitrr.ac.in

Uranium(VI) is one of the most harmful and carcinogenic ion if present in water above its permissible limit. The main objective of this study is removal of uranium(VI) from water sample using nano zerovalent iron prepared by green synthesis approach with the help of *Annacardium occidentale* testa extract in which the whole process is completely environmental friendly and cost effective and does not involve any hazardous chemicals. Size of AO-Fe nanoparticle is characterized through UV-visible spectroscopy and FTIR analysis. Morphology of nanoparticle is studied using SEM-EDS and XRD analysis. The adsorption capacity of AO-Fe nanoparticle is studied using batch experiments. Effect of different parameters are then analyzed such as pH, adsorbent dosage, contact time and U(VI) ion concentration. Adsorption isotherm is also studied using Langmuir and Freundlich adsorption isotherm where correlation constant R^2 is about 0.99.

Keywords: Testa, *Annacardium occidentale*, Uranium(VI), Cashew nuts, Phytochemicals, Polyphenols.

INTRODUCTION

Rapid industrialization and population growth are some of the important reason of great utilization of water and also leads to water crisis. Industries such as dye industries, leather industries, paper industries and many more are required for continuous supply of water for various purposes. Discharge from these bodies contains variety of contaminants which may be toxic [1,2].

Removal of these materials is a great challenge for reutilization of these waters. A wide range of treatment methods such as filtration, UV treatment, adsorption, distillation, ion exchange, precipitation are available now a days [2,3]. Nanotechnology deals with the use of matter to a size of nanoscale having special properties and have various applications [3]. Microscopic particles having a size in between 1-100 nm can be termed as nanoparticles [4]. Due to different optical, thermal, electrical, chemical and physical properties [5], they find a variety of applications in the areas of medicine, chemistry, environment, agriculture, energy, information and communications, heavy industry and consumer goods [6]. Nanotechnology is very effective in water treatment and removal of toxic heavy metals and radioactive elements such as uranium(VI) from it as they are cost effective, environment friendly and highly efficient [7].

Nanomaterials such as zerovalent iron, nickel oxide nanoparticles were reported for the removal of U(VI), heavy metals, hexavalent chromium, arsenate, cadmium, *etc*. [1-9]. Iron nanoparticles are in the same way emerged as nanoparticles used for the removal of radioactive elements like uranium. Metallic iron and iron based materials are well recognized as efficient scavangers of uranium from water [8-11]. Removal has been attributed to both the adsorption of uranyl ions (UO_2^{2-}) on to iron corrosion products [12-15] and the reductive precipitation of soluble U(VI) in to the insoluble U(IV) oxides, driven by coupled corrosion of Fe(0) or Fe(II) [16-20].

EXPERIMENTAL

Analytical reagent grade chemicals are used for synthesis without further purification. $FeCl_3 \cdot 6H_2O$ was purchased from Merck, Germany. Standard stock solution of uranium(VI) 100 µg mL^{-1} in 2-5 % HNO_3 (ICP-MS-66N-0.01X-1, AccuStandard, USA), NaOH and conc. HCl was purchased from Loba Chemie. For making all the solutions and preparation of extract, Merck Millipore water is used.

Green synthesis of AO-Fe nanoparticles from *Anacardium occidentale* testa extract: Extract from the testa of A*nnacardium occidentale* and AO-Fe nanoparticles were prepared as published article [21] with slight modifications. Solid FeCl$_3$·6H$_2$O (1.35 g) was dissolved in 50 mL millipore water to make 0.1 M FeCl$_3$·6H$_2$O solution which was mixed with *Anacardium occidentale* testa extract in the ratio of 4:2 resulting in slight colour change from orange to black. Futher the solution was heated at 70 ºC at 700 rpm in Tarson′s Digital Spinot for 15 min. The resulting solution is centrifuged at 8000 rpm for 30 min in TC 4100F Eltek Research Centrifuge. The precipitate was taken off from supernatant, washed, dried and then kept for further characterization and adsorption studies [21].

The AO-Fe nanoparticles synthesized are characterized using UV-visible spectroscopy (Labtronics Double Beam UV-visible spectrophotometer), FTIR (Cary 630 FTIR, Agilent Technologies), SEM-EDX (ZEISS EVO 18 Scanning Electron Microscope) and XRD (PANalytical 3 kW X′pert Powder-Multifunctional).

Batch experiments: Batch experiments were carried out using uranium(VI) stock solution of 100 ppb, prepared from standard uranium(VI) stock solution of 100 µg mL^{-1}. AO-Fe nanoparticles (0.01 g) was added to 10 mL stock solution prepared at different pH values and placed in rotary shaker. The mixed solution was then filtered through Whatmann filter paper no. 42 and the filtrate was taken to measure the concentration of remaining uranium(VI) in the solution through LED Fluorimeter LF-2a. The removal efficiency of uranium is measured using eqn. 1:

$$R = \frac{C_i - C_f}{C_i} \times 100\ \%$$ (1)

where, C_i (mg L^{-1}) is initial and C_f (mg L^{-1}) is final equilibrium concentration of uranium ion, respectively. The concentration of uranium ion adsorbed per unit mass of AO-Fe nanoparticle is measured using eqn. 2:

$$q_e = \frac{(C_i - C_f)V}{w}$$ (2)

where, q_e (mg g^{-1}) is adsorption capacity at equilibrium, w (g) is the weight of adsorbent and V is the volume of sample.

RESULTS AND DISCUSSION

The colour of extract changes sharply from light orange to black and pH (6.7) of solution also decreases during the synthesis of AO-Fe nanoparticle, which becomes acidic pH of 2.2.

UV-visible analysis: Labtronics Double Beam UV-visible spectrophotometer is used for UV-visible analysis of AO-Fe nanoparticles within range of 220 to 400 nm for determining the reduction of Fe(III) to Fe(0) nanoparticle. Excitation of surface plasmon vibrations results in absorption peak at 292 nm in AO-Fe nanoparticle solution (Fig. 1).

FTIR analysis: In green synthesis of any nanoparticles, functional groups adsorbed on the surface of the nanoparticle during reduction are determined by the FTIR analysis. These are the groups which provide stability to nanoparticles by adsor-
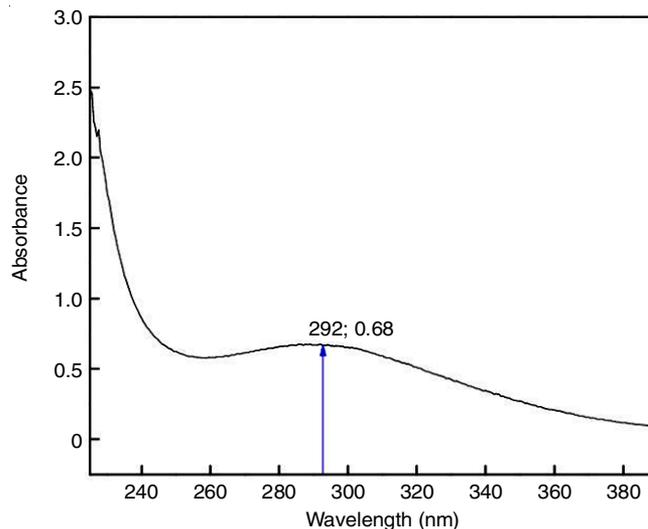
Fig. 1. UV-visible spectra of AO-Fe nanoparticles

ption over its surface. Different phytochemical constituents such as catechin, epicatechin and epigallocatechin and phenolic acids like syringic acid, gallic acid and *p*-coumaric acids are found in *Annacardium occidentale* testa [22-25], which not only reduces Fe(III) to Fe(0) but also gets adsorbed over the surface of nanoparticle formed. Fig. 2 depicts a broad peak at 3298.7 cm^{-1} in the FTIR spectra represents the presence of hydrogen bonded -OH group of polyphenols. These polyphenols adsorbed over the surface of nanoparticle are responsible for reduction and provides stability to the nanoparticle. Various peaks in the FTIR spectra of AO-Fe nanoparticle at 1032.5 and 1080.9 cm^{-1} shows the presence of various alcoholic and carboxylic groups, which acts as capping agents and provides stability.
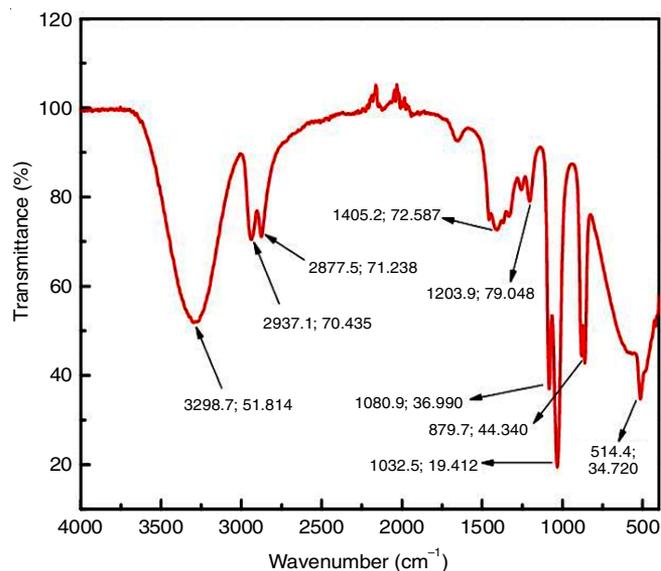
Fig. 2. FTIR spectra of AO-Fe nanoparticles

SEM-EDX analysis: SEM and EDX analysis is done using ZEISS EVO 18 Scanning Electron Microscope. Fig. 3 depicted the SEM and EDX images of AO-Fe nanoparticle, which shows that the nanoparticles are very irregular in shape, scattered and have voids in between them. The average size of nanoparticles is found to be around 70-90 nm.
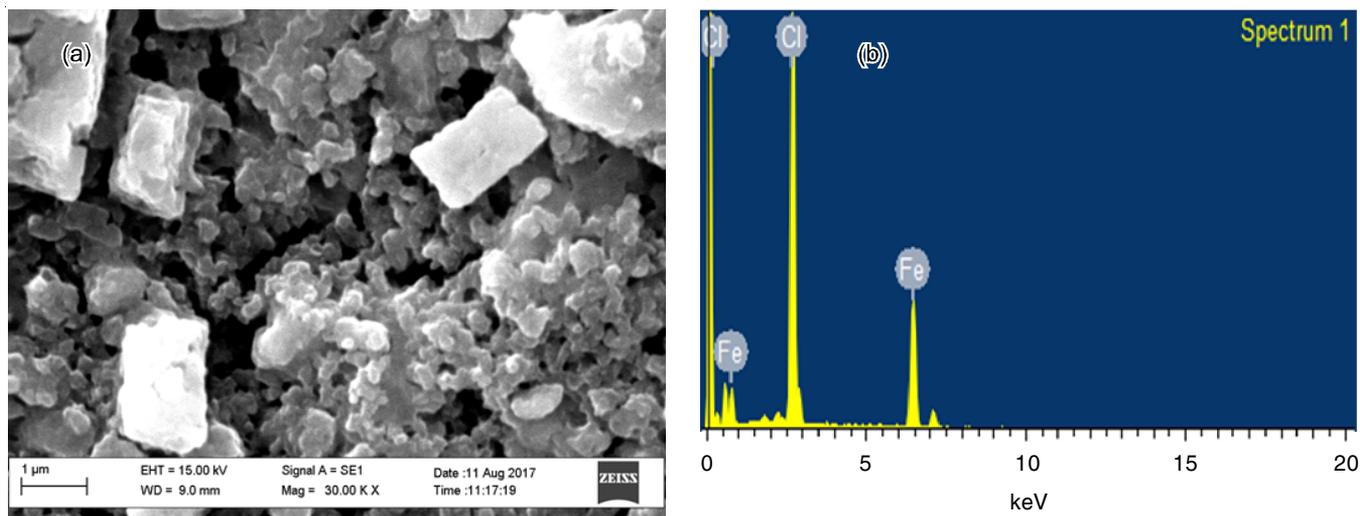
Fig. 3. (a) SEM image of AO-Fe nanoparticles, (b) EDX of AO-Fe nanoparticles

XRD analysis: Fig. 4 showed the mixed diffraction peaks obtained as a result of green synthesis of AO-Fe nanoparticle and formation of layer of polyphenolic groups over the surface of nanoparticle. Two diffraction peaks appears at $2\theta = 42.32°$ and $43.32°$, which corresponds to the formation of AO-Fe nanoparticle.
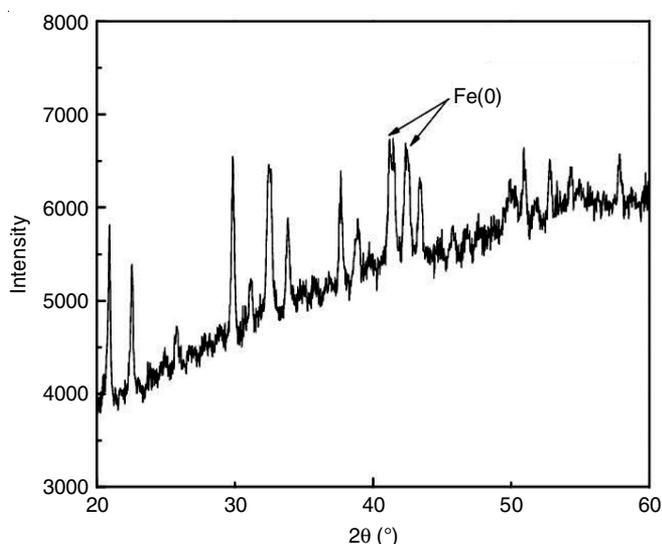
Fig. 4. XRD Pattern of AO-Fe nanoparticle

Removal of U(VI) by AO-Fe nanoparticles: For removal of U(VI) from water samples, water having different concentrations of U(VI) was taken in an Erlenmeyer's flask at different pH values. Different concentrations of AO-Fe nanoparticle was then added to the water sample containing U(VI) and allowed for adsorption in a rotary shaker for different time intervals. All the samples are then filtered through Whatmann filter paper no. 42 and concentration of U(VI) left after adsorption was measured through LED Fluorimeter LF-2a and maximum adsorption peaks were determined.

Effect of adsorbent dosage: The effect of adsorbent dosage was studied by adding varying concentration 0.01-0.07 g of AO-Fe nanoparticles to the water sample having 100 ppb of U(VI). It was observed that the adsorption of U(VI) increases with the increase in the adsorbent dosage until maximum of 0.04 g and then becomes almost constant (Fig. 5a). With increase in adsorbent dosage, more amount of U(VI) ions are adsorbed until the concentration of U(VI) ions decreases which makes its adsorption constant. Hence, 0.04 g amount is the optimum dosage capacity of AO-Fe nanoparticles for U(VI).

Effect of pH: For studying the effect of pH in the adsorption of U(VI) by AO-Fe nanoparticles, water samples containing 100 ppb U(VI) at different pH value from 2-9 pH were taken in Erlenmeyer's flask and its adsorption was studied over AO-Fe nanoparticles. It was observed that the adsorption of U(VI) increases with pH until it reaches pH 4 and then again starts decreasing (Fig. 5b). This shows that acidic conditions exposes more surface for adsorption by reduction of U(VI) through H^+ ions and adsorption is maximum at lower pH [26]. Hence, at optimum pH 4, maximum adsorption of U(VI) takes place from water sample over AO-Fe nanoparticles.

Effect of adsorbate concentration: To study the effect of concentration of U(VI) on adsorption, different water samples with variable U(VI) concentration of 100-300 ppb were taken and 0.04 g of AO-Fe nanoparticle was added and agitated in a rotary shaker. All other parameters were kept constant. It was observed that the percentage removal of U(VI) decreases with increase in the concentration of U(VI) in water samples (Fig. 5c). When the concentration of U(VI) is low, more vacant sites are present in the AO-Fe nanoparticle which further decreases as the concentration of U(VI) increases. Hence, the adsorption of U(VI) and in turn the percentage removal of U(VI) decreases with increase in concentration of U(VI).

Effect of contact time: Effect of contact time in efficient removal of uranium(VI) is studied by taking all the parameters constant and only varying the time of adsorption. Different water samples containing 100 ppb of uranium(VI) were taken in Erlenmeyer's flask and 0.04 g of AO-Fe nanoparticle is added to it and agitated in rotary shaker for different time intervals of 0-180 min. It was observed that as the percentage of removal of U(VI) increases with the increase of time till it reaches a maximum and almost constant value (Fig. 5d). Maximum percentage of U(VI) removal takes place at an optimum contact time of 60 min.
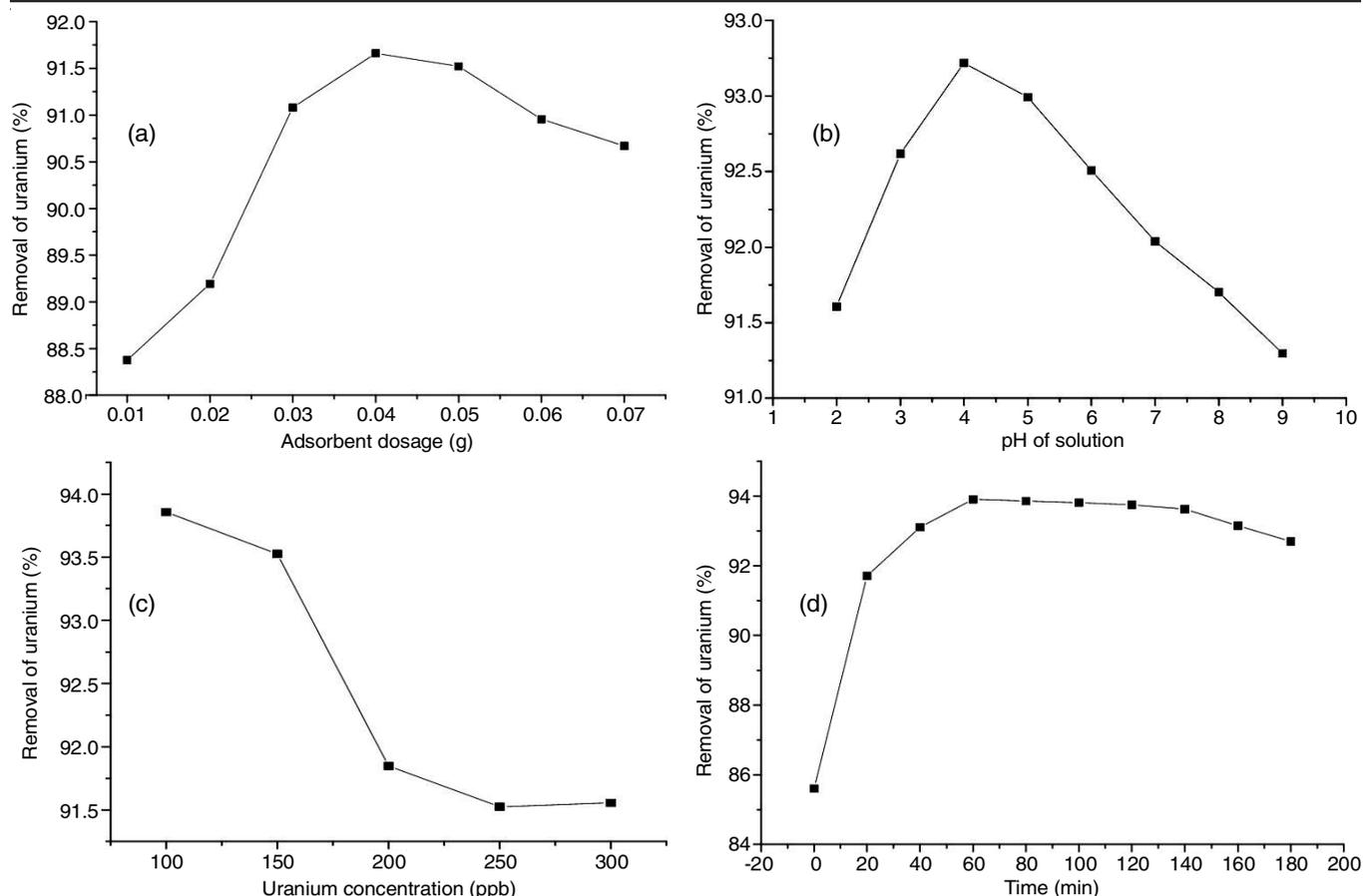
Fig. 5. (a) Effect of adsorbent dosage on adsorption, (b) effect of pH on adsorption, (c) effect of initial concentration of uranium on adsorption, (d) effect of contact time on adsorption

Adsorption isotherms: The relation between the adsorbate concentration and adsorption capacity of adsorbent can be studied with the help of adsorption isotherms *i.e.* Langmuir and Freundlich adsorption isotherms, which determines the adsorption behaviour of the nanoparticles.

Langmuir adsorption isotherm: The Langmuir plot of C_e/q_e *vs.* C_e gives a straight line where $1/Q_o$ is the slope and $1/Q_o b$ is the intercept, which is used for determining the values of Q_o and b. Another essential parameter of Langmuir adsorption isotherm is expressed as dimensionless equilibrium parameter or separation factor (R_L). The value of R_L indicates the favourable or unfavourable nature of the Langmuir plot. If $R_L > 1$, then isotherm is unfavourable, linear ($R_L = 1$), favourable ($0 < R_L < 1$) and irreversible ($R_L = 0$). Value of R_L is 0.1, which indicates that the adsorption is favourable.

Freundlich adsorption isotherm: Freundlich adsorption isotherm indicates the multilayer adsorption for heterogenous surfaces. A Freundlich adsorption plot of log q_e *vs.* log C_e gives a straight line with slope 1/n and intercept of log K_f which are used for determining the parameters n and K_f. The high value of regression coefficient ($R^2 = 0.99$) in both Langmuir and Freundlich adsorption isotherms also suggests that both iso-

therms better describes the adsorption of U(VI) by AO-Fe nanoparticles (Table-1).

Conclusion

Green synthesis of AO-Fe nanoparticles is an environment friendly process of synthesis of nanoparticles as it employs waste product of the cashew plant *i.e.* testa of *Annacardium occidentale* (AO) and also the method of synthesis does not involve any harmful chemicals or precursors. These AO-Fe nanoparticles are in turn stable as the phytochemical constituents in extract acts as capping agents for providing stability and are further used for the nanosorption of uranium(VI) from water. The AO-Fe nanoparticles are effective nanosorptive agents for removal of U(VI) from water at optimized conditions of pH 4 with 93-94 % removal of U(VI) in 60 min of contact time. Adsorption isotherms with $R_L = 0.1$ and $R^2 = 0.99$ also indicates that the isotherms fitted well to the experimental data.

TABLE-1
LANGMUIR AND FREUNDLICH ADSORPTION PARAMETERS FOR ADSORPTION OF URANIUM OVER AO-Fe NANOPARTICLES

Ion	Langmuir				Freundlich		
	Q_0	b	R_L	R^2	n	k_f	R^2
U(VI)	11.61	1.06	0.1	0.99	9.25	16.470	0.99

CONFLICT OF INTEREST

The authors declare that there is no conflict of interests regarding the publication of this article.

REFERENCES

1. G. Crini, *Prog. Polym. Sci.*, **30**, 38 (2005);
   https://doi.org/10.1016/j.progpolymsci.2004.11.002.
2. G. Gangadhar, U. Maheshwari and S. Gupta, *Nanosci. Nanotechnol.-Asia*, **2**, 140 (2012);
   https://doi.org/10.2174/2210681211202020140.
3. Environmental Protection Agency, Nanotechnology White Paper, USEPA 100/B-07/001 (2007).
4. K.N. Thakkar, S.S. Mhatre and R.Y. Parikh, *Nanomedicine*, **6**, 257 (2010);
   https://doi.org/10.1016/j.nano.2009.07.002.
5. S. Panigrahi, S. Kundu, S. K. Ghosh, S. Nath and T. Pal, *J. Nanopart. Res*., **6**, 411 (2004);
   https://doi.org/10.1007/s11051-004-6575-2.
6. The Energy and Resources Institute, Nanotechnology Development in India: Building Capability and Governing the Technology, Briefing Paper, TERI, New Delhi, India (2010).
7. Patanjali, Pooja, R. Singh, A. Kumar and P. Chaudhary, eds.: A.K. Shukla and S. Iravani, Nanotechnology for Water Treatment: A Green Approach, In: Green Synthesis, Characterization and Applications of Nanoparticles, Elsevier Inc. (2019).
8. C.D. Hsi and D. Langmuir, *Geochim. Cosmochim. Acta*, **49**, 1931 (1985);
   https://doi.org/10.1016/0016-7037(85)90088-2.
9. J.J. Lenhart and B.D. Honeyman, *Geochim. Cosmochim. Acta*, **63**, 2891 (1999);
   https://doi.org/10.1016/S0016-7037(99)00269-0.
10. T.B. Scott, Ph.D. Thesis, Sorption of Uranium onto Iron Bearing Minerals, Interface Analysis Centre, University of Bristol, Bristol, U.K. (2005).
11. T.B. Scott, O. Riba and G.C. Allen, *Geochim. Cosmochim. Acta*, **71**, 5044 (2007);
    https://doi.org/10.1016/j.gca.2007.08.017.
12. J.N. Fiedor, W.D. Bostick, R.J. Jarabek and J. Farrell, *Environ. Sci. Technol*., **32**, 1466 (1998);
    https://doi.org/10.1021/es970385u.
13. J. Farrell, W.D. Bostick, R.J. Jarabek and J.N. Fiedor, *Ground Water*, **37**, 618 (1999);
    https://doi.org/10.1111/j.1745-6584.1999.tb01150.x.
14. T.B. Scott, G.C. Allen, P.J. Heard and M.G. Randell, *Geochim. Cosmochim. Acta*, **69**, 5639 (2005);
    https://doi.org/10.1016/j.gca.2005.07.003.
15. T.B. Scott, G.C. Allen, P.J. Heard, A.C. Lewis and D.F. Lee, *Proc. R. Soc. A*, **461**, 1247 (2005);
    https://doi.org/10.1098/rspa.2004.1441.
16. K.J. Cantrell, D.I. Kaplan and T.W. Wietsman, *J. Hazard. Mater*., **42**, 201 (1995);
    https://doi.org/10.1016/0304-3894(95)00016-N.
17. L. Charlet, E. Liger and P. Gerasimo, *J. Environ. Eng*., **124**, 25 (1998);
    https://doi.org/10.1061/(ASCE)0733-9372(1998)124:1(25).
18. B. Gu, L. Liang, M.J. Dickey, X. Yin and S. Dai, *Environ. Sci*., **21**, 3366 (1998);
    https://doi.org/10.1021/es980010o.
19. E. Liger, L. Charlet and P. van Cappellen, *Geochim. Cosmochim. Acta*, **63**, 2939 (1999);
    https://doi.org/10.1016/S0016-7037(99)00265-3.
20. S.J. Morrison, D.R. Metzler and C.E. Carpenter, *Environ. Sci. Technol*., **35**, 385 (1998);
    https://doi.org/10.1021/es001204i.
21. C. Chandra, F. Khan and D.K. Verma, *Int. J. Eng. Technol. Sci. Res.*, **4**, 671 (2017).
22. N. Chandrasekara and F. Shahidi, *J. Agric. Food Chem*., **59**, 5006 (2011);
    https://doi.org/10.1021/jf2000772.
23. N. Chandrasekara and F. Shahidi, *Food Chem*., **129**, 1388 (2011);
    https://doi.org/10.1016/j.foodchem.2011.05.075.
24. A.G. Mathew, H.A.B. Parpia, *J. Food Sci*., **35**, 140 (1970);
    https://doi.org/10.1111/j.1365-2621.1970.tb12123.x.
25. J. Trox, V. Vadivel, W. Vetter, W. Stuetz, D.R. Kammerer, R. Carle, V. Scherbaum, U. Gola, D. Nohr and H.K. Biesalski, *Food Chem*., **128**, 1094 (2011);
    https://doi.org/10.1016/j.foodchem.2011.04.018.
26. J. Yang, X. Wang, M. Zhu, H. Liu and J. Ma, *J. Hazard. Mater.*, **264**, 269 (2014);
    https://doi.org/10.1016/j.jhazmat.2013.11.037.